J|A|C|S COMMUNICATIONS

Published on Web 07/09/2009

Macroporous Silicon Oxycarbide Fibers with Luffa-like Superhydrophobic Shells

Ping Lu,[†] Qing Huang,*[,‡] Baodan Liu,[§] Yoshio Bando,[§] You-Lo Hsieh,[†] and Amiya K. Mukherjee*[,‡]

Fiber and Polymer Science, University of California, Davis, California 95616, Department of Chemical Engineering and Materials Science, University of California, Davis, California 95616, and International Center for Materials Nanoarchitectonics (MANA), National Institute for Material Science, Tsukuba, 305-0044, Japan

Received April 14, 2009; E-mail: hqhuang@ucdavis.edu; akmukherjee@ucdavis.edu

Porous nanostructured materials systems have been well-established and widely employed as catalyst supporters, molecular sieves, gas adsorbents, and ceramics.[1] Covalent-bonded porous inorganic materials, such as C and BN,[2,3] are highly sought after in high temperature applications, aimed to enhance the thermal stability, thermal conductivity, and chemical tolerance that are still unmet in amorphous mesoporous silica. Silicon oxycarbide (SiOC) ceramics, for example, are stable in their microstructure and composition in air even at temperatures up to 1200 °C.[4,5] The underlying mechanism for this excellent resistance to oxidation has been attributed to the existence of a graphene network which sequesters the nanodomains of SiOC clusters and inhibits their diffusion rate.[6] Although SiOC ceramic foams and bicontinuous porous architectures have been recently fabricated,[7,8] their resultant specific surface areas are yet to match those of mesoporous silica. Herein, we report a feasible synthetic approach without using any template to obtain macroporous SiOC ceramic fibers with a high specific surface area.

The primary method to form porous ceramics is a reverse replication process where either channels preformed by templating block copolymers or spaces among compacted colloidal particles are infiltrated with a ceramic polymeric precursor. This process either needs stringent requirements of chemical compatibility between the ceramic precursor and copolymer templates in case of destruction of self-assembled soft microstructures[9] or demands size-controllable ordered silica nanoparticles as rigid templates to confine the final ceramic hierarchical structures. For instance, a macroporous silicon carbonitride monolith has been achieved by capillary filling of packed beds of polystyrene or silica spheres with preceramic polymers.[10] Recently, a single-source ceramic precursor containing a hybrid block polymer of polynorbornene−decaborane was synthesized to enable the direct formation of ordered ceramic nanostructures.[11] Although the replicate-template approach is viable, identifying an appropriately versatile template for a ceramic polymeric precursor has remained elusive. Therefore, a more feasible route is highly desirable to realize their application in industrial scale.

Polyureasilazane (PUS) is a low-viscous thermoset material for polymer-derived and silicon-based covalent ceramics. It dissolves in a nonproton solvent, such as THF or DMF, while having the ability to be slowly cross-linked at temperatures above 180 °C. In the current study, PUS was homogeneously cured into isolated solid nanoparticles by the aid of a peroxide catalyst in a poly(methyl methacrylate) (PMMA) matrix after the PUS/PMMA solution was electrospun into continuous fibers (Supporting Information (SI)). A scanning electron microscope (SEM) image taken on a cross section of a typical as-spun fiber shows obvious phase separation where nanoparticles are uniformly distributed in a PMMA fiber (Figure S1). Subsequent calcination in nitrogen at a moderate temperature of 500 °C atmosphere transformed the polymer fibers to solid-state fibers (Figure 1a). Near 100% PMMA polymer that was weakly associated with the nanoparticles or that filled the interstitial spacing was driven off. Meanwhile, the cross-linked PUS polymer lost 19.7 wt % from the escape of volatile ammonia, hydrogen, and hydrocarbons (such as methane) during pyrolysis (see thermogravimetric analysis in Figure S2). Calcination also results in fusion of adjacent fibers (Figures 1a and S3), the degree of which has implications for achieving a three dimensionally macroporous fiber network.

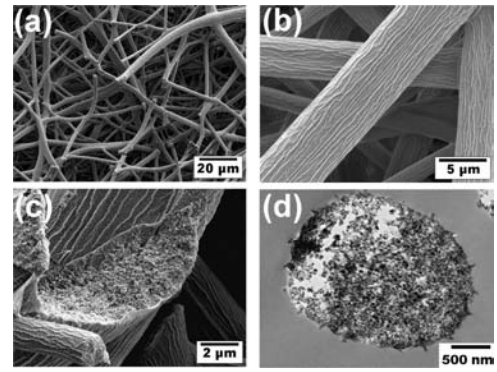

Figure 1. SEM images of (a) as-calcined fibers, (b) their luffa-like surface pattern, and (c) a cross section showing compacted nanoparticles. (d) TEM image of a thin section also reveals capsulated nanoparticles forming a macroporous fiber.

The SEM images illustrate the resultant fibers with a patterned shell structure which are filled by compacted nanoparticles (Figure 1b and 1c). Transmission electron microscope (TEM) observations on cross sections of sliced fibers along both the radial and axial directions clearly show the encapsulated and tightly compacted nanoparticles that have an average diameter of 50 nm (Figures 1d and S4). Elemental mapping images and line-scan spectra collected by the energy-dispersive X-ray spectrometer both manifest the even distribution of Si, C, and O elements in 2D and 1D projections (Figures S5 and S6), respectively, reconfirming the same composition in core and shell regions. Electron energy-loss spectroscopy that is more sensitive to the detection of light elements presents no N signal, further corroborating the product to be a kind of silicon oxycarbide material (Figure S7). There is no crystalline phase formed in the product which can be identified by X-ray diffraction spectra (Figure S8), so this fiber is a glass-like amorphous material. It is worth noting that the absence of nitrogen in the product is attributed to the sensitivity of the PUS precursor to humidity and oxygen that are inevitable when all experiments were performed

[†] Fiber and Polymer Science, University of California.
[‡] Department of Chemical Engineering and Materials Science, University of California.
[§] National Institute for Material Science.

10.1021/ja902757a CCC: $40.75

in an ambient environment. However, as-calcined SiOC fibers can be thermodynamically doped by nitrogen through heat treatment in an ammonia atmosphere at 1000 °C, while the macroporous architecture in fibers was well preserved after substitution of N for C in the backbone of fibers (Figures S9 and S10).

Chemical structures of macroporous fibers were analysized by a ^{29}Si solid state nuclear magnetic resonance (NMR) technique to disclose the local environment of silicon atoms (Figure S11). The peaks at −66.5 and −57.9 ppm attributed to $(SiO_3)SiCH_3$ and $(SiO_2)SiCH_3OH$ structural units, respectively, have a mole ratio of 4:1, which accurately gives the chemical formula $SiO_{1.77}C_{0.59}$. These chemical groups were also identified in Fourier transform infrared spectroscopy (Figure S12), which determined the hydrophobic property of fibers to be described below.

The formation of a luffa-like "skin" and the capsulated nanoparticle core is very intriguing. Here we provide a tentative explanation. In the core region, the gaseous species (such as low-molecular-weight carbohydrate gases) generated from the decomposition of PMMA which accounts for 75 wt % of as-spun fibers would have quickly accumulated to form voids that separated the cured SiOC nanoparticles, which was followed by a process of rearrangement of the nanoparticles to reduce voids. This accommodation process leads to a marked volume shrinkage of fibers. However, on the surface or shell, void formation is kinetically unfavorable since gases formed can be instantly released to the environment. Therefore, neighboring SiOC nanoparticles on the surface undergo a further condensation reaction and finally form a dense layer or "skin" as observed. This loose "skin" had to be wrinkled to follow the contracted core volume, leading to an appearance of longitudinal striations because of the limited shrinkage ratio along the axial direction when compared to the radial direction.

N_2 adsorption/desorption measurement of as-calcined SiOC fibers presents a type IV isotherm hysteresis loop (Figure 2a),[12] indicating the exclusive existence of large nanopores which are the result of interparticle voids formed from the removal of PMMA polymer. The specific surface area calculated by the Brunauer−Emmett−Teller (BET) method and the pore volume determined by the Barrett−Joyner−Halenda (BJH) approach are 391 $m^2\ g^{-1}$ and 0.56 $cm^3\ g^{-1}$, respectively. The BJH adsorption pore sizes range from 10 to 100 nm and center at 50 nm (Figure 2b). All these pores are interconnected as shown in TEM images (Figure S4a and S4b) and can be accessible to the gas and liquid phases in potential service applications.

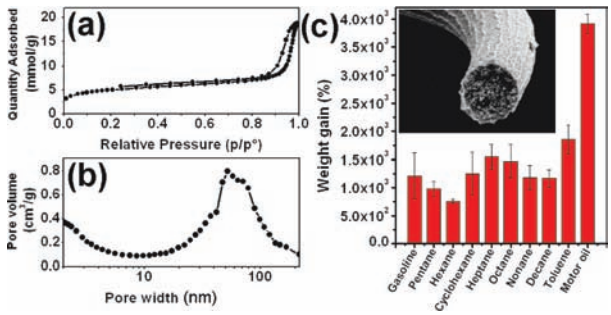

Figure 2. Nitrogen adsorption/desorption isotherm hysteresis loop (a) and pore size distribution (b) of as-calcined SiOC fibers. Uptake capacities of fiber mat for a series of organic solvents and oils in terms of its weight gain (c), inset showing a typical SiOC "straw" filled by oleophilic nanoparticles.

Patterned surfaces have been shown to improve the superhydrophobicity of already hydrophobic materials as the well-known Lotus effect does.[13] The water contact angle measured on the as-calcined fibers is 156°. A water drop can suspend on a fiber mat and easily roll down at a small tilt angle (less than 10°, as seen in Figure S13a). Even when fibers were repeatedly annealed at high temperature, such a superhydrophobic surface remains stable and shows no degradation in structure or composition. Meanwhile, the macroporous fibers show an exceptional ability to uptake oil or organic solvents (Figure 13b). A series of alkanes with 5 (pentane) to 10 (decane) carbons were tested, and their weights absorbed are more than 10 times that of the macroporous fibers used (Figure 2c). More specifically, a weight gain of 39 times was achieved for motor oil, indicating this superhydrophobic fiber is a promising candidate as a suction skimmer in marine oil-spill recovery.[14] Dynamic absorption measurement indicates such suction processes to be within 0.02 s (Figure S14). The unique oil capsulation by such enveloped macroporous fibers not only accounts for the observed excellent uptake capacity but also shows the improved retention capacity when compared to normal fibers which lose half of the initial absorbed oil or organic solvents.[15]

The above-described silicon oxycarbide macroporous fibers present an alternate route to fabricate a high-surface-area nanostructure through in situ cross-linking of a preceramic precursor without using a prepattern template. The unique luffa-like shell combining with silicon-containing groups accounts for their superhydrophobicity. Meanwhile, oil-uptake capacity of the corresponding macroporous fiber mat is superior to that of solid fiber membranes due to its oil-preservable inner porous structure. Such a refractory inorganic macroporous fiber is also capable of supporting catalysts, such as ruthenium nanoparticles, to convert ammonia to hydrogen for green energy applications more efficiently at elevated temperature.[10]

Acknowledgment. A.K.M. and Q.H. are thankful for support from the U.S. National Science Foundation (Grant CMMI #0700272); Y.L.H. and P.L. are thankful for support from the National Textile Center (Project M02-CD05) and the Jastro-Shields Graduate Research Award at the University of California at Davis, CA, USA.

Supporting Information Available: Experimental procedure and characterization including XRD, SEM, TEM, EELS, EDS, FTIR, ^{29}Si NMR, nitrogen adsorption isotherm data and dynamic absorption curve for macroporous SiOC fibers. This material is available free of charge via Internet at http://pubs.acs.org.

References

(1) Colombo, P. *Science* **2008**, *322*, 381–83.
(2) Kruk, M.; Jaroniec, M.; Ryoo, R.; Joo, S. H. *J. Phys. Chem. B* **2000**, *104*, 7960–68.
(3) Dibandjo, P.; Bois, L.; Chassagneux, F.; Cornu, D.; Letoffe, J. M.; Toury, B.; Babonneau, F.; Miele, P. *Adv. Mater.* **2005**, *17*, 571–74.
(4) Renlund, G. M.; Prochazka, S.; Doremus, R. H. *J. Mater. Res.* **1991**, *6*, 2723–34.
(5) Pantano, C. G.; Singh, A. K.; Zhang, H. X. J. *Sol-gel Sci. Technol.* **1999**, *14*, 7–25.
(6) Scarmi, A.; Soraru, G. D.; Raj, R. J. *Non-Cryst. Solids* **2005**, *351*, 2238–43.
(7) Colombo, P.; Bernardo, E. *Compos. Sci. Technol.* **2003**, *63*, 2353–59.
(8) Chan, V. Z. H.; Hoffman, J.; Lee, V. Y.; Iatrou, H.; Avgeropoulos, A.; Hadjichristidis, N.; Miller, R. D.; Thomas, E. L. *Science* **1999**, *286*, 1716–19.
(9) Pauletti, A.; Handjani, S.; Fernandez-Martin, C.; Gervais, C.; Babonneau, F. J. *Ceram. Soc. Jpn.* **2008**, *116*, 449–53.
(10) Sung, I. K.; Christian; Mitchell, M.; Kim, D. P.; Kenis, P. J. A. *Adv. Funct. Mater.* **2005**, *15*, 1336–42.
(11) Malenfant, P. R. L.; Wan, J. L.; Taylor, S. T.; Manoharan, M. *Nat. Nanotechnol.* **2007**, *2*, 43–46.
(12) Rouquerol, J.; Avnir, D.; Fairbridge, C. W.; Everett, D. H.; Haynes, J. H.; Pernicone, N.; Ramsay, J. D. F.; Sing, K. S. W.; Unger, K. K. *Pure Appl. Chem.* **1994**, *66*, 1739–58.
(13) Marmur, A. *Langmuir* **2004**, *20*, 3517–19.
(14) Yuan, J. K.; Liu, X. G.; Akbulut, O.; Hu, J. Q.; Suib, S. L.; Kong, J.; Stellacci, F. *Nat. Nanotechnol.* **2008**, *3*, 332–36.
(15) Wei, Q. F.; Mather, R. R.; Fotheringham, A. F.; Yang, R. D. *Mar. Pollut. Bull.* **2003**, *46*, 780–83.

JA902757A